

## Tidal Tails of Minor Mergers: Star Formation Efficiency in the Western Tail of NGC 2782

Karen Knierman

*School of Earth & Space Exploration, Arizona State University, 550 E. Tyler Mall, Room  
PSF-686 (P.O. Box 871404), Tempe, AZ 85287-1404*

karen.knierman@asu.edu

Patricia M. Knezek

*WIYN Consortium, Inc., 950 North Cherry Avenue, Tucson, AZ 85719*

pknezek@noao.edu

Paul Scowen

*School of Earth & Space Exploration, Arizona State University, 550 E. Tyler Mall, Room  
PSF-686 (P.O. Box 871404), Tempe, AZ 85287-1404*

paul.scowen@asu.edu

Rolf A. Jansen<sup>1</sup>

*School of Earth & Space Exploration, Arizona State University, 550 E. Tyler Mall, Room  
PSF-686 (P.O. Box 871404), Tempe, AZ 85287-1404*

rolf.jansen@asu.edu

Elizabeth Wehner

*Department of Astronomy, Haverford College, Haverford, PA 19041*

ewehner@haverford.edu

### ABSTRACT

---

<sup>1</sup>Department of Physics, 550 E. Tyler Mall, Room PSF-470 (P.O.Box 871504), Tempe, AZ 85287-1504

While major mergers and their tidal debris are well studied, they are less common than minor mergers (mass ratios  $\lesssim 0.3$ ). The peculiar spiral NGC 2782 is the result of a merger between two disk galaxies with a mass ratio of  $\sim 4 : 1$  occurring  $\sim 200$  Myr ago. This merger produced a molecular and HI rich, optically bright Eastern tail and an HI-rich, optically faint Western tail. Non-detection of CO in the Western Tail by Braine et al. (2001) suggested that star formation had not yet begun to occur in that tidal tail. However, deep H $\alpha$  narrowband images show evidence of recent star formation in the Western tail. Across the entire Western tail, we find the global star formation rate per unit area ( $\Sigma_{\text{SFR}}$ ) several orders of magnitude less than expected from the total gas density. Together with extended FUV+NUV emission from *Galaxy Evolution Explorer* along the tail, this indicates a low global star formation efficiency in the tidal tail producing lower mass star clusters. The HII region we observed has a *local* (few-kpc scale)  $\Sigma_{\text{SFR}}$  from H $\alpha$  that is less than that expected from the *total* gas density, which is consistent with other observations of tidal debris. The star formation efficiency of this HII region inferred from the total gas density is low, but normal when inferred from the molecular gas density. These results suggest the presence of a very small, locally dense region in the Western tail of NGC 2782 or of a low metallicity and/or low pressure star forming region.

*Subject headings:* galaxies: interactions — galaxies: individual (NGC 2782)

## 1. Introduction

Major mergers of spiral galaxies are known to create structures such as tidal dwarf galaxies (TDGs) and star clusters within their debris (e.g., Duc et al. 2000; Weilbacher et al. 2002; Knierman et al. 2003; Mullan et al. 2011). While examples of major mergers are well known (e.g., NGC 4038/9 “The Antennae”; Whitmore et al. 1999), interactions between equal mass galaxies are relatively rare compared to minor mergers (mass ratios of  $\lesssim 0.3$ ). As part of a larger study, we aim to understand how these frequent encounters shape galactic structure and probe star formation in gas that may be marginally stable. Previous work studied how neutral hydrogen may affect star cluster formation in tidal debris (Maybhate et al. 2006; Mullan et al. 2011), but studies of molecular gas in tidal debris have focused on larger episodes of star formation such as those resulting in the formation of TDGs (Braine et al. 2001). This work examines star formation on smaller scales in the tidal debris of the minor merger NGC 2782.

NGC 2782, a peculiar spiral at a distance of  $(39.5 \pm 2.8)$  Mpc<sup>1</sup>, is undergoing a nuclear

starburst (Devereux 1989). Smith (1994) used a restricted three-body dynamical model to show that NGC 2782 is the result of a merger of two disk galaxies with a mass ratio of  $\sim 0.25$  occurring  $\sim 200$  Myr ago. It has two tidal tails: an Eastern tail which has a concentration of HI and CO at its base and a gas-poor optically bright knot  $2.7'$  from the center; and an HI-rich, optically faint Western tail (Smith 1994). Mullan et al. (2011) in their  $V$  and  $I$  band *Hubble Space Telescope*/WFPC2 survey of tidal tails find 87 star cluster candidates in the Eastern tail of NGC 2782 and 10 candidates in the Western tail.

Non-detection of CO at the location of HI knots in the Western tail led Braine et al. (2001) to argue that the HI “has presumably not had time to condense into  $H_2$  and for star formation to begin.” However, if this tail was pulled from the lower metallicity outer regions of the spiral galaxy like TDGs (Duc et al. 2000) or the merged dwarf galaxy, the lower metallicity may affect the conversion factor between CO and  $H_2$  and result in an underestimated molecular mass. It is possible for  $H_2$  to be present despite CO being undetected. While the blue colors in the Western tail suggest that it formed from the disruption of the dwarf companion, the  $m_{\text{HI}}/L_B$  ratios suggest that some gas must have originated in NGC 2782’s gaseous disk and is therefore mixed composition (Wehner 2005).

We obtained new  $H\alpha$  observations to determine the star formation efficiency in the Western tail of NGC 2782. Section 2 presents observations, calibration, and results. In Section 3, we discuss global and local star formation in the tail and relate it to star formation in general.

## 2. Observations

Images in  $UBVR$  and  $H\alpha$  were taken with the Loral 2K CCD imager at the Lennon 1.8m Vatican Advanced Technology Telescope (VATT) ( $6.4'$  field of view,  $0.375''$  pixel $^{-1}$ ).  $H\alpha$  images ( $6\times 1200$ s) used an 88 mm Andover three-cavity interference filter ( $\lambda_c=6630\text{\AA}$ ; FWHM= $70\text{\AA}$ ). We observed the tail in Kron-Cousins  $R$  ( $3\times 300$ s) to allow continuum subtraction, following Lee (2006). Images were reduced using standard IRAF<sup>1</sup> tasks. The inset in Figure 1 shows the continuum-subtracted  $H\alpha$  image that contained the only  $H\alpha$  emission-line source detected at more than  $10\sigma$  in the Western tail.

---

<sup>1</sup>From NED, corrected for Virgo, Great Attractor, and Shapley, which we will use for the duration of this paper. Smith (1994); Braine et al. (2001) use distances of 34 Mpc and 33 Mpc, respectively.

<sup>1</sup>IRAF is distributed by the National Optical Astronomy Observatory, which is operated by the Association of Universities for Research in Astronomy, Inc., under cooperative agreement with the National Science Foundation.

## 2.1. H $\alpha$ calibration

We calibrated our H $\alpha$  images using observations of 3–5 spectrophotometric standard stars from (Oke 1990). Zeropoints were obtained by comparing the integral over the filter response function of their spectral energy distribution and the instrumental magnitude from aperture photometry. Extinction corrections assumed a standard atmospheric extinction coefficient of 0.08 mag airmass<sup>-1</sup> (Lee 2006). The dispersion of the zeropoints from individual standard stars was typically 0.02 mag.

Following Lee (2006), we removed the contribution to the H $\alpha$  flux of the [NII] doublet ( $\lambda$ 6548,6583) and emission line flux from the  $R$  filter. We used an empirical relation between metallicity and the [NII]/H $\alpha$  ratio from Figure 9 of van Zee et al. (1998). For a metallicity of  $0.4Z_{\odot}$ ,  $12 + \log(\text{O}/\text{H}) = 8.06$  gives  $\log([\text{NII}]/\text{H}\alpha) = -1.3$ , from which follows the H $\alpha$  flux.

## 2.2. Results

The H $\alpha$  observations yielded a detection of one source in the Western tail centered on  $\alpha = 9:13:51.2$ ,  $\delta = +40:08:07$  (see Figure 1) with  $L_{\text{H}\alpha} = (1.9 \pm 0.3) \times 10^{39}$  erg s<sup>-1</sup>. For comparison, this HII region is fainter than the massive star cluster 30 Dor ( $L_{\text{H}\alpha} = 6 \times 10^{39}$  erg s<sup>-1</sup>), but > 1000 times brighter than Orion with its handful of O-stars ( $L_{\text{H}\alpha} = 10^{36}$  erg s<sup>-1</sup>). It is consistent with the formation of a large star cluster. This HII region has also been detected by Bournaud et al. (2004) and, recently, by Werk et al. (2011). The HII region is located  $\sim 20''$  away, but well within the  $55''$  half power beam size, from the location where Smith et al. (1999) searched for CO(1-0).

## 3. Discussion

We compare the star formation rate (SFR) per unit area ( $\Sigma_{\text{SFR}}$ ) from H $\alpha$  to that obtained from the observed gas density using the Kennicutt law, and the SFE in the tail to that seen in other tidal debris, normal galaxies, and starbursts.  $\Sigma_{\text{SFR}}$  from H $\alpha$  for the whole tail is much less than expected given the observed gas density. With only one H $\alpha$  region in the tail, the derived  $\Sigma_{\text{SFR}}$  is a lower limit, as most of the stars forming are late B and A stars based on ultraviolet emission. This indicates that there is a lower SFE in the tail resulting in the formation of fewer high mass stars. Star formation on the few-kpc scale represents a  $\Sigma_{\text{SFR}}$  that is less than expected from the Kennicutt law, using the total gas surface density and the observed H $\alpha$ . Since the original Kennicutt law was formulated using observations of spiral disks, this indicates that the star formation in the tail is less

efficient than in spiral disks. Using the molecular gas depletion time, the SFE of the HII region is similar to the tidal debris regions of Arp 158 and normal galaxies but lower than observed in starburst galaxies. Using only the HI gas as a tracer of the available material, the SFE is higher than seen in the outer disks of spiral galaxies. Given a low SFE from the total gas and a normal SFE from the molecular gas, the observed HII region may be a very small, locally dense region. The lack of observed CO emission could be due to destruction of molecular gas by FUV, effects of beam dilution, the influence of low metallicity on the CO-H<sub>2</sub> conversion factor, or a low pressure gas environment.

The SFR from H $\alpha$  is (Equation (2) in Kennicutt 1998):  $\text{SFR} (M_{\odot}\text{yr}^{-1}) = 7.9 \times 10^{-42} L(\text{H}\alpha) (\text{ergs s}^{-1})$ . The expected SFR from the gas surface density is (Equation (7) in Kennicutt 1998):

$$\Sigma_{\text{SFR}}(\text{gas}) = 2.5 \times 10^{-4} \left( \frac{\Sigma_{\text{gas}}}{1 M_{\odot}\text{pc}^{-2}} \right)^{1.4} M_{\odot}\text{yr}^{-1}\text{kpc}^{-2} \quad (1)$$

Table 1 compares the global and local SFR in the Western tail: tail location, area of HI clump or entire tail, H $\alpha$  SFR with error, SFR per unit area from H $\alpha$  ( $\Sigma_{\text{SFR}}(\text{H}\alpha)$ ) with error, mass of HI, mass of molecular gas, total gas surface density, and SFR per unit area from gas density ( $\Sigma_{\text{SFR}}(\text{gas})$ ).

### 3.1. Star Formation on Global Scales

Using the entire area of Western tail of NGC 2782, the global  $\Sigma_{\text{SFR}}(\text{H}\alpha) = 9 \times 10^{-6} M_{\odot}\text{yr}^{-1}\text{kpc}^{-2}$  is three orders of magnitude below the expected  $\Sigma_{\text{SFR}}(\text{gas}) < 5 \times 10^{-3}$

Table 1. Comparison of Star Formation Rates in Western Tail of NGC 2782

Location	Area (kpc <sup>2</sup> )	H $\alpha$ SFR ( $M_{\odot}\text{yr}^{-1}$ )	$\Sigma_{\text{SFR}}(\text{H}\alpha)$ ( $M_{\odot}\text{yr}^{-1}\text{kpc}^{-2}$ )	$M_{\text{HI}}^{\text{a}}$ ( $10^8 M_{\odot}$ )	$M_{\text{mol}}^{\text{b}}$ ( $10^8 M_{\odot}$ )	$\Sigma_{\text{gas}}^{\text{c}}$ ( $M_{\odot}\text{pc}^{-2}$ )	$\Sigma_{\text{SFR}}(\text{gas})^{\text{d}}$ ( $M_{\odot}\text{yr}^{-1}\text{kpc}^{-2}$ )
HI-N	8.6	< 0.0003	< 0.00003	0.73	< 0.086 <sup>e</sup>	< 12.9	< 0.006
HI-mid	14.7	0.015(.002)	0.001(0.0002)	1.15	< 0.16 <sup>f</sup>	< 12.2	< 0.005
HI-S	19.3	< 0.0003	< 0.00002	1.16	< 0.16 <sup>f</sup>	< 9.4	< 0.004
W Tail	2300	0.015	0.000009	20	< 0.4 <sup>e,f</sup>	< 11.7	< 0.005

(a) Smith (1994), corrected for distance, (b)  $M_{\text{mol}}$  inferred from CO observations, (c) Includes helium ( $M_{\text{gas}} = 1.36(M_{\text{HI}} + M_{\text{H}_2})$ ) (d) From Kennicutt (1998),  $\Sigma_{\text{gas}}$  includes only HI and H<sub>2</sub> (e) Braine et al. (2001), corrected for distance, (f) Smith et al. (1999), corrected for distance

$M_{\odot}\text{yr}^{-1}\text{kpc}^{-2}$ . The  $\Sigma_{\text{SFR}}(\text{H}\alpha)$  is also three orders of magnitude lower than those typical for spiral and dwarf galaxies, but there is a significant dilution factor due to the large area of the tidal tail and low density of stars and gas therein.

The Magellanic Stream is a local example of a gas tail of presumed tidal origin with no star formation. Putman et al. (2003) measured the total HI gas mass in the Stream to be  $2.1 \times 10^8 M_{\odot}$ . By converting the angular size of the Stream ( $100^{\circ} \times 10^{\circ}$ ) to projected physical size using a distance of 55 kpc (Putman et al. 2003), we infer an area of  $940.9 \text{ kpc}^2$ . Using the resulting gas surface density of  $\Sigma_{\text{HI}} = 2.2 \times 10^5 M_{\odot}\text{kpc}^{-2}$ , the Magellanic Stream has an expected  $\Sigma_{\text{SFR}} = 3 \times 10^{-5} M_{\odot}\text{yr}^{-1} \text{ kpc}^{-2}$ , two orders of magnitude lower than the Western tail of NGC 2782.

The difference between the  $\Sigma_{\text{SFR}}$  values indicates a lower SFE. However, the SFR is a lower limit since there is one HII region and H $\alpha$  represents star formation in the last 5 Myr. Also the SFR in the tail could be higher than inferred from H $\alpha$  if it is predominately of a Taurus-Auriga type (Kenyon et al. 2008), producing few star clusters with high mass stars. If so, the color would be blue, but no H $\alpha$  would be observed. To examine this further, FUV and NUV images of NGC 2782 from the *Galaxy Evolution Explorer* (*GALEX*) All-sky Imaging Survey (AIS; Morrissey et al. 2007) were inspected. As seen in Figure 2, faint UV emission is detected along the Western tidal tail, indicating the presence of young stellar populations, likely dominated by B and A stars. Since there is no H $\alpha$  emission (except for the single knot) the star clusters forming along the tail were likely of low mass and had a negligible probability of forming early B and O stars.

### 3.2. Star Formation on Local Scales

We also examine star formation within Western tail HI regions. Smith (1994) measured 10 massive HI clumps with masses from  $3 \times 10^7 M_{\odot}$  to  $1.8 \times 10^8 M_{\odot}$ . Only three of these HI clumps have star cluster candidates (Mullan et al. 2011). Since only one HII region was found in the Western tail, we use the H $\alpha$  detection limit as a limit for the high-mass SFR for the other two regions. The crosses in Figure 1 show the location of these HI clumps with their SFR in Table 1.

The star formation on few-kpc scales associated with the HII region is lower than expected from the Kennicutt law.  $\Sigma_{\text{SFR}}$  calculated from the H $\alpha$  luminosity is  $0.001 \pm 0.0002 M_{\odot}\text{yr}^{-1}\text{kpc}^{-2}$ . Due to the non-detection of CO in the Western tail and using a standard CO to H $_2$  conversion factor, we are only able to establish upper limits to the SFR from the gas density of  $\Sigma_{\text{SFR}}(\text{gas}) < 0.005 M_{\odot}\text{yr}^{-1} \text{ kpc}^{-2}$ . While follow-up spectroscopy is necessary to

determine the composition of the gas in the Western tail of NGC 2782, TDGs in major mergers are shown to have  $\sim 0.3Z_{\odot}$  (Duc et al. 2000). The standard CO to H<sub>2</sub> conversion factor ( $\alpha_{\text{CO1-0}} = 4.3 \text{ M}_{\odot}(\text{K km s}^{-1} \text{ pc}^2)^{-1}$ ) is based on observations of the Milky Way. Using galaxies with  $z \leq 1$ , Genzel et al. (2012) find a linear relation given by  $\log \alpha_{\text{CO1-0}} = 12.1 - 1.3\mu_0$  where  $\mu_0 = 12 + \log(\text{O}/\text{H})$ . For a metallicity of  $0.3Z_{\odot}$  (or  $\mu_0 = 8.19$ ), the appropriate conversion factor is  $\alpha_{\text{CO1-0}} = 27.5 \text{ M}_{\odot}(\text{K km s}^{-1} \text{ pc}^2)^{-1}$  giving a factor of six higher molecular mass limit ( $M_{\text{mol}} \leq 6 \times 10^7 \text{ M}_{\odot}$ ) than that from the standard conversion factor ( $M_{\text{mol}} \leq 9 \times 10^6 \text{ M}_{\odot}$ ). This would then give a larger expected  $\Sigma_{\text{SFR}}(\text{gas}) < 0.01 \text{ M}_{\odot}\text{yr}^{-1} \text{ kpc}^{-2}$  and would give an even larger difference from the measured H $\alpha$  SFR. Boquien et al. (2011) use multi-wavelength data of Arp 158 to study the local Schmidt-Kennicutt law in a merger. They find that star forming regions in the tidal debris follow a different Schmidt-Kennicutt law than those in the central regions of the merger, falling along a line of similar slope to Daddi et al. (2010), but offset so that the same gas density gives lower values of SFR. Plotting our HII region in the Western tail of NGC 2782 on Figure 6 of Boquien et al. (2011), we find it to be consistent with quiescent star formation as seen in the tidal debris of Arp 158. This may indicate that star formation in tidal debris is less efficient than that in the central regions of mergers and in normal galaxies.

However, this HII region has a normal SFE using the molecular gas limit. The depletion timescale of the molecular gas is calculated by  $\tau_{\text{dep,H}_2} = M_{\text{mol}}/\text{SFR}$ . For the HII region in the western tail of NGC 2782,  $\tau_{\text{dep}} < 1 \text{ Gyr}$  which is comparable to the molecular gas depletion timescales determined for the star forming regions in Arp 158 ( $\tau_{\text{dep}} \sim 0.5 - 2 \text{ Gyr}$ ; Boquien et al. 2011) and in TDGs ( $\tau_{\text{dep}} \sim 0.8 - 4 \text{ Gyr}$ ; Braine et al. 2001). These ranges are also similar to the average gas depletion timescales in spiral galaxies. The inverse of  $\tau_{\text{dep}}$  is related to the star formation efficiency. For the HII region in the western tail of NGC 2782,  $\text{SFE} = (\tau_{\text{dep}})^{-1} > 9.3 \times 10^{-10} \text{ yr}^{-1}$ . In contrast to the low SFE implied from the total gas density, this HII region appears to have a similar SFE to the tidal tail regions in Arp 158 and in normal spiral galaxies based on the molecular gas upper limit but lower than dense starburst nuclei (e.g., NE region in Arp 158; Boquien et al. 2011). Bigiel et al. (2010) find very low SFE ( $< 9 \times 10^{-11} \text{ yr}^{-1}$ ) in the outer disks of spiral galaxies using FUV and HI observations. The HII region in the western tail of NGC 2782 has a higher SFE than these outer disk regions ( $(\tau_{\text{dep,HI}})^{-1} = 1.3 \times 10^{-10} \text{ yr}^{-1}$ ) using only the HI gas mass.

Since there is a low SFE using the total gas density and a normal SFE using the molecular gas limit, this HII region may be very small and dense or something else entirely. Due to the lack of wide-spread *massive* star formation, using H $\alpha$  as the star formation indicator likely underestimates the true nature of star formation in the Western tidal tail. This means that our SFE estimates are lower limits, particularly when combined with the upper limit on the molecular gas mass. The discrepancies between the SFE may indicate

that there is a denser region of star forming gas that is too small to have been observed. Unlike the very dense regions in the central regions of mergers such as those in the models of Teyssier et al. (2010), there may still be elevated levels of star formation across mergers even out in the tidal debris regions. Star formation in mergers likely depends on local conditions at a scale of 1 kpc, which is the size of the gravitational instabilities in the ISM of mergers and the injection scale of turbulence (Elmegreen 1993; Elmegreen & Scalo 2004).

### 3.3. Impact on Star Formation

Tidal tails provide laboratories for star formation under conditions very different from quiescent galaxy disks. With low gas pressures and densities and small amounts of stable molecular gas they are perhaps at the edge of the parameter space open to star formation. The Western tail of NGC 2782 is HI gas rich, but CO is not observed in the massive HI knots in the tail. This study finds an HII region in the tidal tail indicating recent star formation. Clearly, the lack of *observable* CO does not guarantee the absence of recent star formation. The presence of a young star cluster in a tail without detectable molecular gas requires one of two situations; either there is no CO, or it escapes detection at the sensitivity of current instrumentation.

If the molecular gas is absent, it may be because it is short-lived. This is most likely the result of a strong ambient FUV radiation field produced by the high local SFR. However, the Western tail does not have a high SFR, so this is unlikely to cause the lack of observed molecular gas.

The molecular cloud may be too small to be observed. In general, H<sub>2</sub> is not directly detectable, so we must rely on surrogate tracers such as CO (Solomon & Vanden Bout 2005, and references therein). At the distance of NGC 2782, an arcsecond corresponds to a physical scale of 190 pc. This is not an unusual size for molecular clouds in the Galaxy; compact clouds may be smaller still. The IRAM observations of Braine et al. (2001) had a 21" half power beam size for their CO(1-0) observations while the Kitt Peak 12m observations of Smith et al. (1999) had a 55" half power beam size. If there are only one or a few clouds at the location of their observations, then beam dilution is a major detriment to the detection of CO at the HII region and in the massive HI clouds.

Physics also works against the detection of molecular gas. If the gas is drawn from the dwarf or the outer regions of the large galaxy, it may be deficient in heavy elements. The CO to H<sub>2</sub> conversion factor can be different for lower metallicities, meaning a larger H<sub>2</sub> mass for a given CO flux. Also, CO does not form in a molecular cloud until  $A_V \geq 3$ , while H<sub>2</sub>



forms at  $A_V < 1$  (Hollenbach & Tielens 1997). In a low pressure environment such as low gas density tidal debris, a substantial amount of molecular gas can exist at low  $A_V$  that will not be detectable through CO. Theoretical models (Wolfire et al. 2010) show that the fraction of molecular mass in the “dark gas” ( $H_2$  and  $C^+$ ) is  $f \sim 0.3$  for typical galactic molecular clouds, increasing for lower  $A_V$  and lower metallicity.

#### 4. Conclusions

While the molecular gas rich Eastern tail of NGC 2782 was known to form stars, we report the detection of recent star formation in the HI rich but molecular gas poor Western tail. This is contrary to the conclusion of Braine et al. (2001) that the lack of detected molecular gas in the Western tail implies that no stars are forming there. Globally, we find that  $\Sigma_{\text{SFR}}$  based on our  $H\alpha$  observations is several orders of magnitude less than expected from the  $HI + H_2$  gas density.  $H\alpha$  observations provide only a lower limit on current SFRs, as *GALEX* observations show extended FUV+NUV emission along the tail. This indicates star formation is less efficient across the tail, forming lower mass star clusters. We find that the observed *local*  $\Sigma_{\text{SFR}}$  from  $H\alpha$  is  $\sim 20\%$  of that expected from the local total gas density, consistent with that observed in the tidal debris of Arp 158. The HII region has a low SFE considering the *total* gas density, but a normal SFE considering the low molecular gas density. This HII region in the Western tail of NGC 2782 may be a very small, dense region the molecular gas in which is not observable with current instruments or may be indicative of star formation in low metallicity and/or low pressure regimes.

We acknowledge helpful comments from the referee, discussions with Janice Lee, Shoko Sakai, Jose Funes, and Jacqueline Monkiewicz, and Rob Kennicutt for use of his narrow-band filter. KK was supported by the University of Arizona/NASA Space Grant Graduate Fellowship and through the NASA Herschel Science Center. We used the NASA/IPAC Extragalactic Database (NED) which is operated by JPL, California Institute of Technology, under NASA contract. This work is based on observations with the Vatican Advanced Technology Telescope (VATT): the Alice P. Lennon Telescope and the Thomas J. Bannan Astrophysics Facility.

#### REFERENCES

Bigiel, F., Leroy, A., Walter, F., Blitz, L., Brinks, E., de Blok, W.J.G., & Madore, B. 2010, *AJ*, 140, 1194

- Boquien, M., Lisenfeld, U., Duc, P.-A., Braine, J., Bournaud, F., Brinks, E., & Charmandaris, V. 2011, *A&A*, 533, 19
- Bournaud, F., Duc, P.-A., Amram, P., Combes, F., Gach, J.-L. 2004, *A&A*, 425, 813
- Braine, J., Duc, P.-A., Lisenfeld, U., et al. 2001, *A&A*, 378, 51
- Daddi, E., Elbaz, D., Walter, F., et al. 2010, *ApJL*, 714, 118
- Devereux, N. A. 1989, *ApJ*, 346, 126
- Duc, P.-A., Brinks, E., Springel, V., Pichardo, B., Weilbacher, P., & Mirabel, I. F. 2000, *AJ*, 120, 1238
- Elmegreen, B.G. 1993, *ApJ*, 419, L29
- Elmegreen, B.G., & Scalo, J. 2004, *ARA&A*, 42, 211
- Genzel, R., Tacconi, L.J., Combes, F., et al. 2011, *ApJ*, 746, 69
- Hollenbach, D.J., & Tielens, A.G.G.M. 1997, *ARA&A*, 35, 179
- Kennicutt, R.C. 1998, *ARA&A*, 36, 189
- Kenyon, S. J., Gomez, M., & Whitney, B. A. 2008, in *Handbook of Star Forming Regions*, Volume I, ed. B. Reipurth, (The Northern Sky ASP Monograph, Vol. 4; San Francisco, CA: ASP), 405
- Knierman, K. A., Hunsberger, S. D., Gallagher, S. C., Charlton, J. C., Whitmore, B. C., Kundu, A., Hibbard, J. E., & Zaritsky, D. 2003, *AJ*, 126, 1227
- Lee, J. 2006, Ph.D. Thesis, University of Arizona
- Maybath, A., Masiero, J., Hibbard, J. E., Charlton, J. C., Palma, C., Knierman, K., & English, J. 2007, *MNRAS*, 381, 59
- Morrissey, P., Conrow, T., Barlow, T., et al. 2007, *ApJS*, 173, 682
- Mullan, B., Konstantopoulos, I.S., Kepley, A.A., et al. 2011, *ApJ*, 731, 93
- Oke, J. B. 1990, *AJ*, 99, 1621
- Putman, M. E., Staveley-Smith, L., Freeman, K. C., Gibson, B. K., & Barnes, D. G. 2003, *ApJ*, 586, 170

- Smith, B. 1994, *AJ*, 107, 1695
- Smith, B., Struck, C., Kenney, J.D.P., & Joglee, S. 1999, *AJ*, 117, 1237
- Solomon, P.M., & Vanden Bout, P.A. 2005, *ARA&A*, 43, 677
- Teyssier, R., Chapon, D., & Bournaud, F. 2010, *ApJL*, 720, 149
- van Zee, L., Salzer, J.J., Haynes, M.P., O'Donoghue, A.A., & Balonek, T.J. 1998, *AJ*, 116, 2805
- Wehner, E. 2005, Ph.D. Thesis, University of Wisconsin - Madison
- Weilbacher, P. M., Fritze-v.Alvensleben, U., Duc, P.-A., & Fricke, K. J. 2002, *ApJ*, 579, L79
- Werk, J. K., Putman, M.E., Meurer, G., R., Santiago-Figueroa, N. 2011, *ApJ*, 735, 71
- Whitmore, B., Zhang, Q., Leitherer, C., Fall, S.M., Schweizer, F., & Miller, B. 1999, *AJ*, 118, 1551
- Wolfire, M., Hollenbach, D., & McKee, C. F., 2010, *ApJ*, 716, 1191

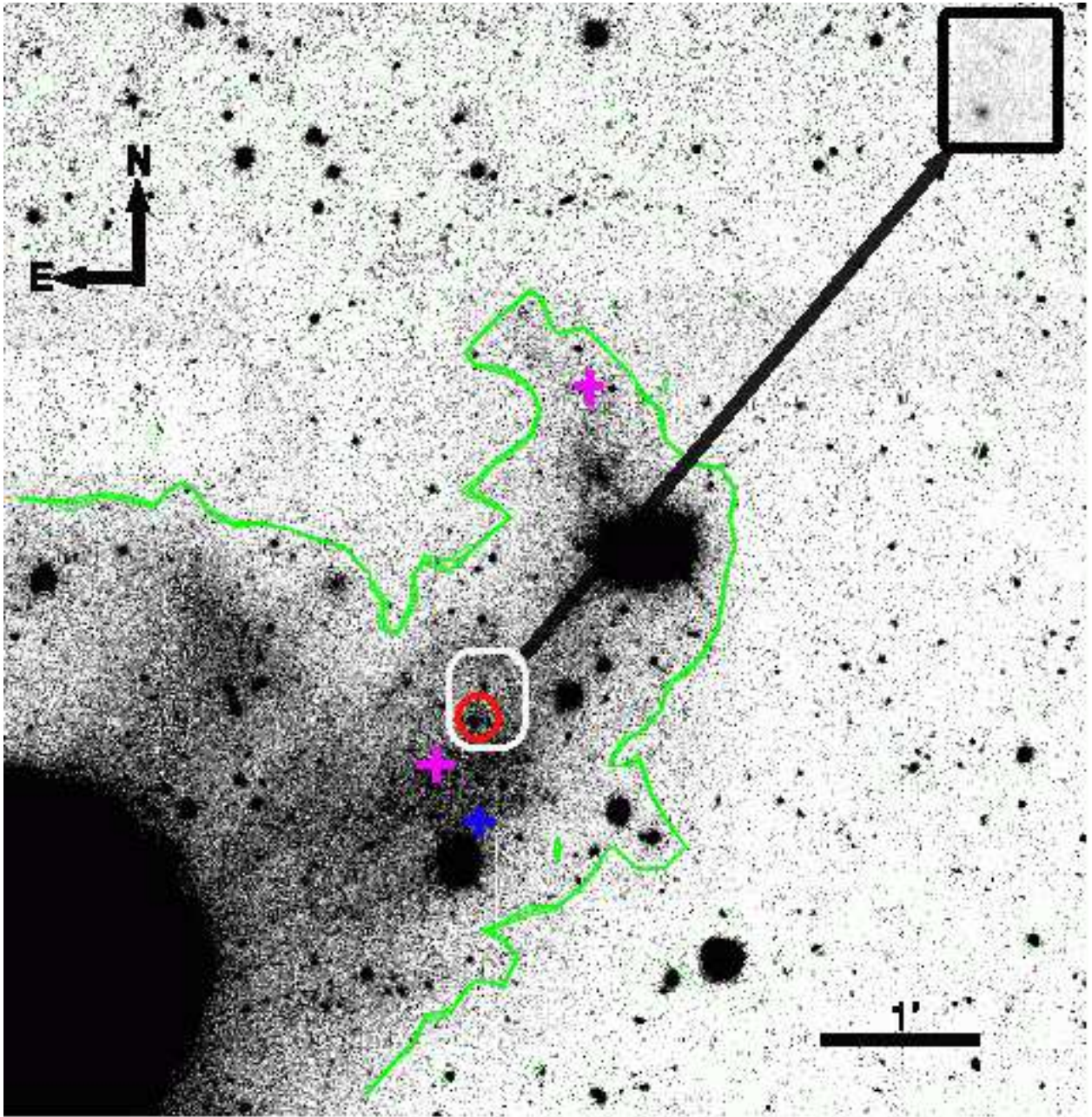


Fig. 1.—  $V$  image of Western tail of NGC 2782. The green contour indicates the area defined as the Western Tidal Tail. Red circle marks the location of the  $H\alpha$  source. The crosses mark the locations of massive HI clouds (Smith 1994). Magenta crosses mark the locations of CO observations from Braine et al. (2001) for the north location and Smith et al. (1999) for the south location. The inset image is the continuum subtracted  $H\alpha$  image of area indicated in the white box.

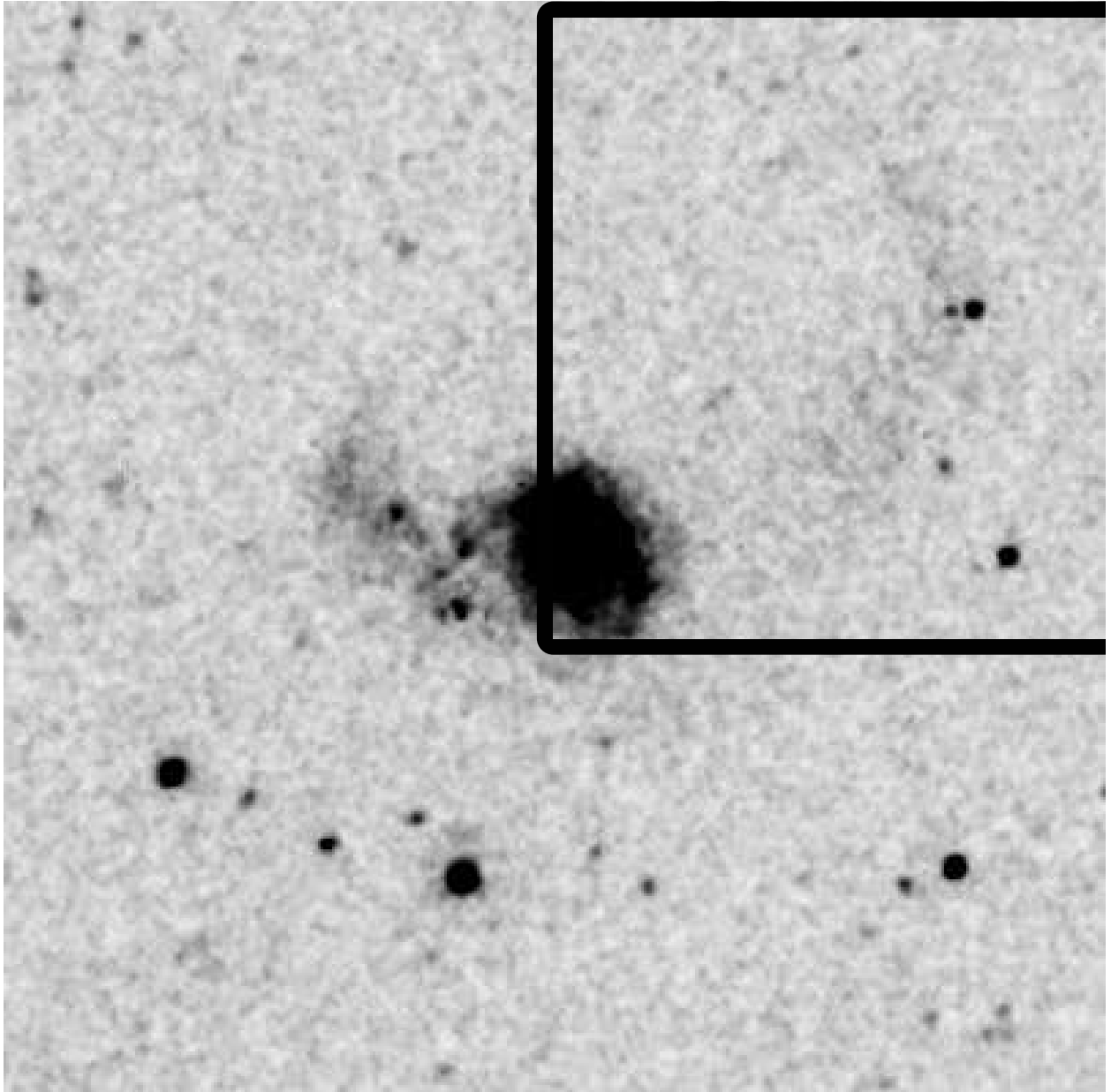


Fig. 2.— Galex composite image of NGC 2782. The box indicates the region covered by the optical image of Fig. 1